SUPPORTING INFORMATION

Threading Through Macrocycles Enhances the Performance of Carbon Nanotubes as Polymer Fillers

Alejandro López-Moreno,[†] Belén Nieto-Ortega,[†] Maria Moffa,[‡] Alberto de Juan,[†] M. Mar Bernal,[†] Juan P. Fernández-Blázquez,[§] Juan J. Vilatela,[§] Dario Pisignano[,‡,¥] and Emilio M. Pérez*[†]*

† IMDEA Nanoscience, C/Faraday 9, Ciudad Universitaria de Cantoblanco, 28049, Madrid, Spain.

‡ Istituto Nanoscienze-CNR, Euromediterranean Center of Nanomaterial Modelling and Technology (ECMT), via Arnesano, 73100, Lecce, Italy.

§ IMDEA Materials, Eric Kandel 2, Getafe, 28005, Madrid, Spain.

¥ Dipartimento di Matematica e Fisica "Ennio De Giorgi", Università del Salento, via Arnesano,Lecce, Italy.

Characterization of MINTs samples

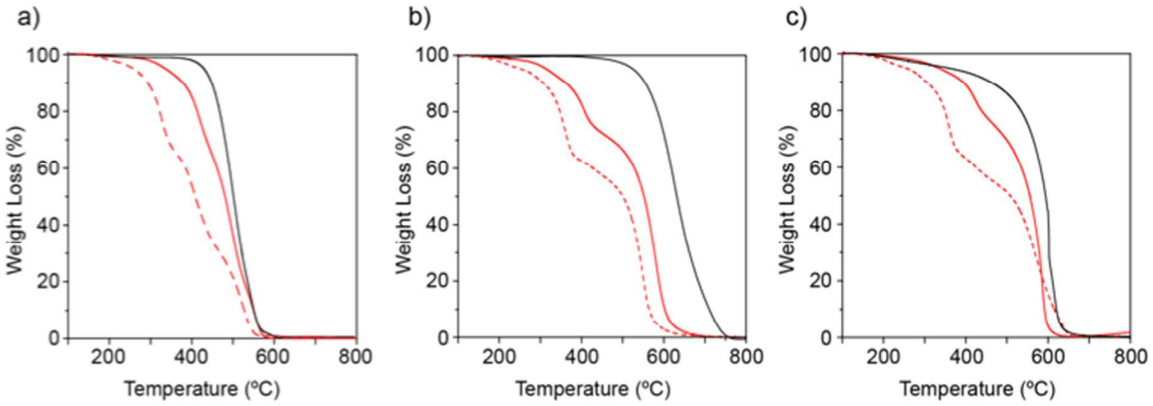

Figure S1. TGA analysis of: a) pristine (6,5)-SWNTs (black), MINT$_{(6,5)}$-**1** (red) and MINT$_{(6,5)}$-**2** (dashed red); b) pristine pp-SWNTs (black), MINT$_{(pp)}$-**1** (red) and MINT$_{(pp)}$-**2** (dashed red). TGAs were run in air at a heating rate of 10 ºC min^{-1}.

TGA of the solid thus obtained showed weight losses of 33% and 41% for MINT$_{(6,5)}$-**1** and MINT$_{(6,5)}$-**2**, 25% and 35% for MINT$_{(pp)}$-**1** and MINT$_{(pp)}$-**2** at approximately 400°C and 26% and 36% for MINT$_{(pp)}$-**1** and MINT$_{(pp)}$-**2.**

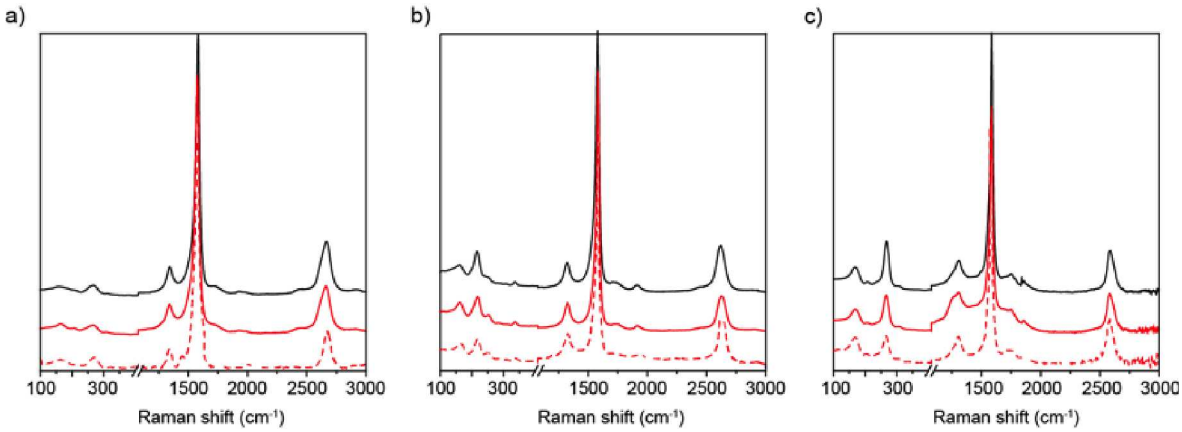

Figure S2. Raman spectra of o-SWNTs (black), MINT$_{(o)}$-**1** (red) and MINT$_{(o)}$-**2** (dashed red): a) λ_{exc} = 532 nm; b) λ_{exc} = 633 nm and c) λ_{exc} = 785 nm All spectra are the average of ten different measurements.

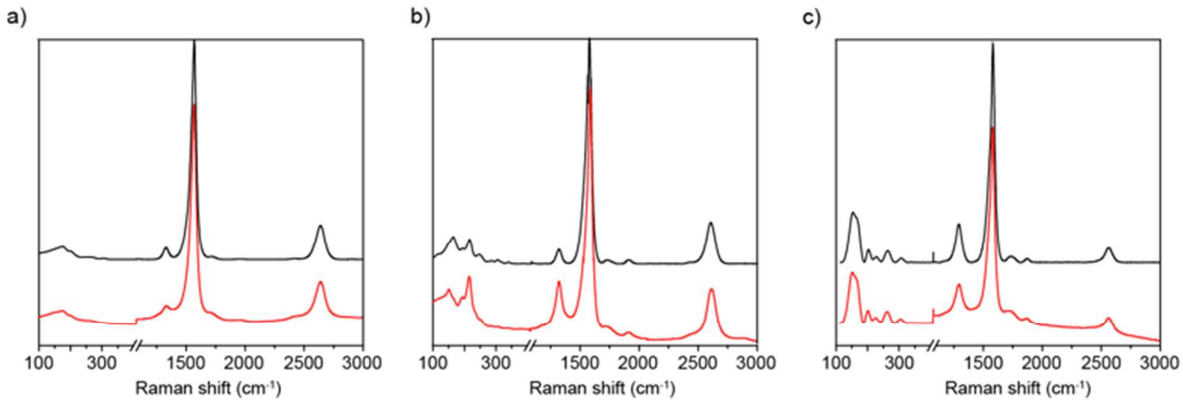

Figure S3. Raman spectra of pp-SWNTs (black) and MINT$_{(pp)}$-**1** (red): a) λ_{exc} = 532 nm; b) λ_{exc} = 633 nm and c) λ_{exc} = 785 nm All spectra are the average of ten different measurements.

Raman spectroscopy (Fig. S2 and S3, λ_{exc} = 532, 633, and 785 nm) reveals no changes in the spectra with respect to pristine pp-SWNTs and o-SWNTs, as expected for the noncovalent functionalization of SWNTs. In particular, we observed no significant increase in the I_D/I_G ratio and no modification in the RBM intensity, which confirmed that there is no covalent modification of the SWNTs.

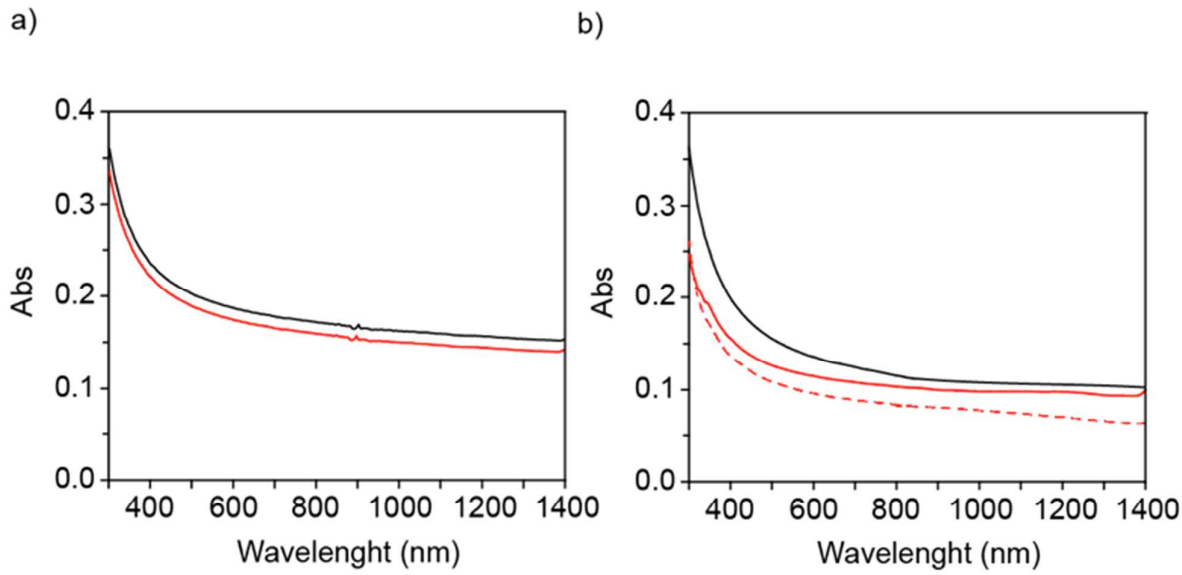

Figure S4. UV/Vis spectra (D_2O, 1% sodium dodecyl sulfate (SDS) , 298 K) of a) pristine pp- SWNTs (black) and $MINT_{(pp)}$-**1** (red); b) o-SWNTs (black), $MINT_{(o)}$-**1** (red) and $MINT_{(o)}$-**2** (dashed red).

In the absorption spectra (D_2O, 1% sodium dodecyl sulphate, 298 K, Fig. S4), the UV region is dominated by the nanotube absorption in both samples, and the characteristic absorption of pyrenes and exTTF in the 300–350 nm and 300-450 nm range respectively is not distinguishable, save for an increase in the relative absorption in this region.

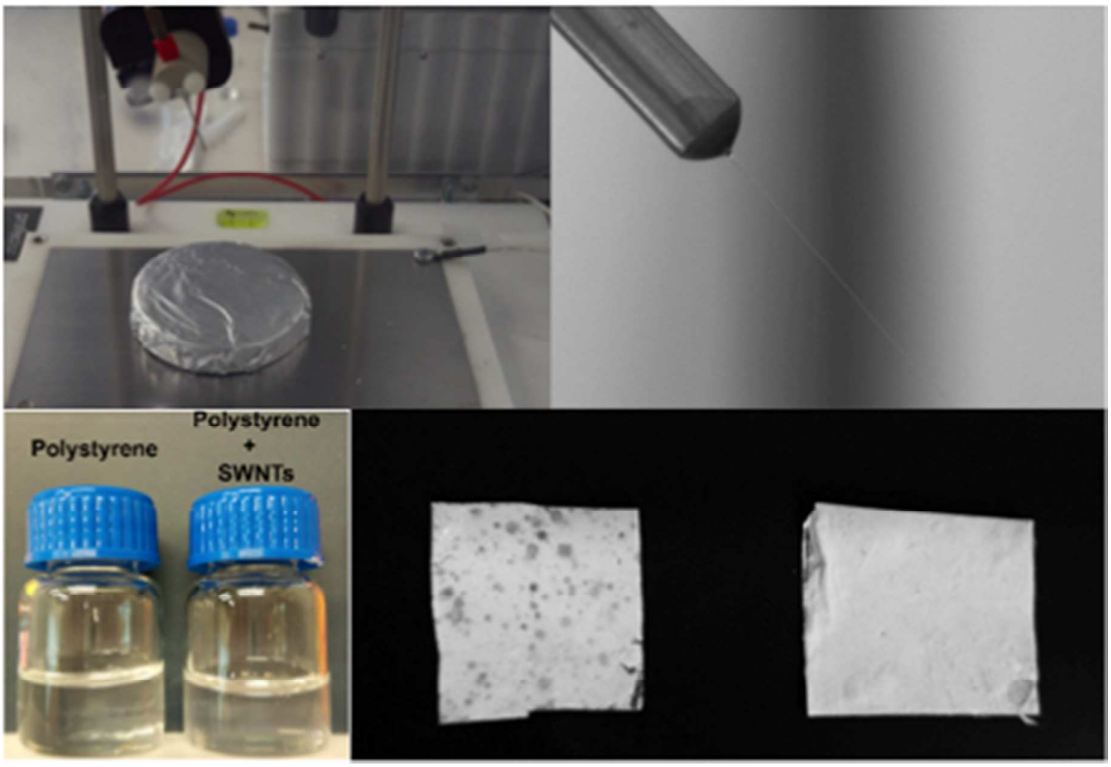

Figure S5. Top Left: Electrospinning setup. Top right: Fiber formation in the needle. Bottom left: Polystyrene and polystyrene/ SWNTs solutions in DMF. Bottom: Defective samples of fibers due to a high concentration of SWNTs (left) and a low fiber density.

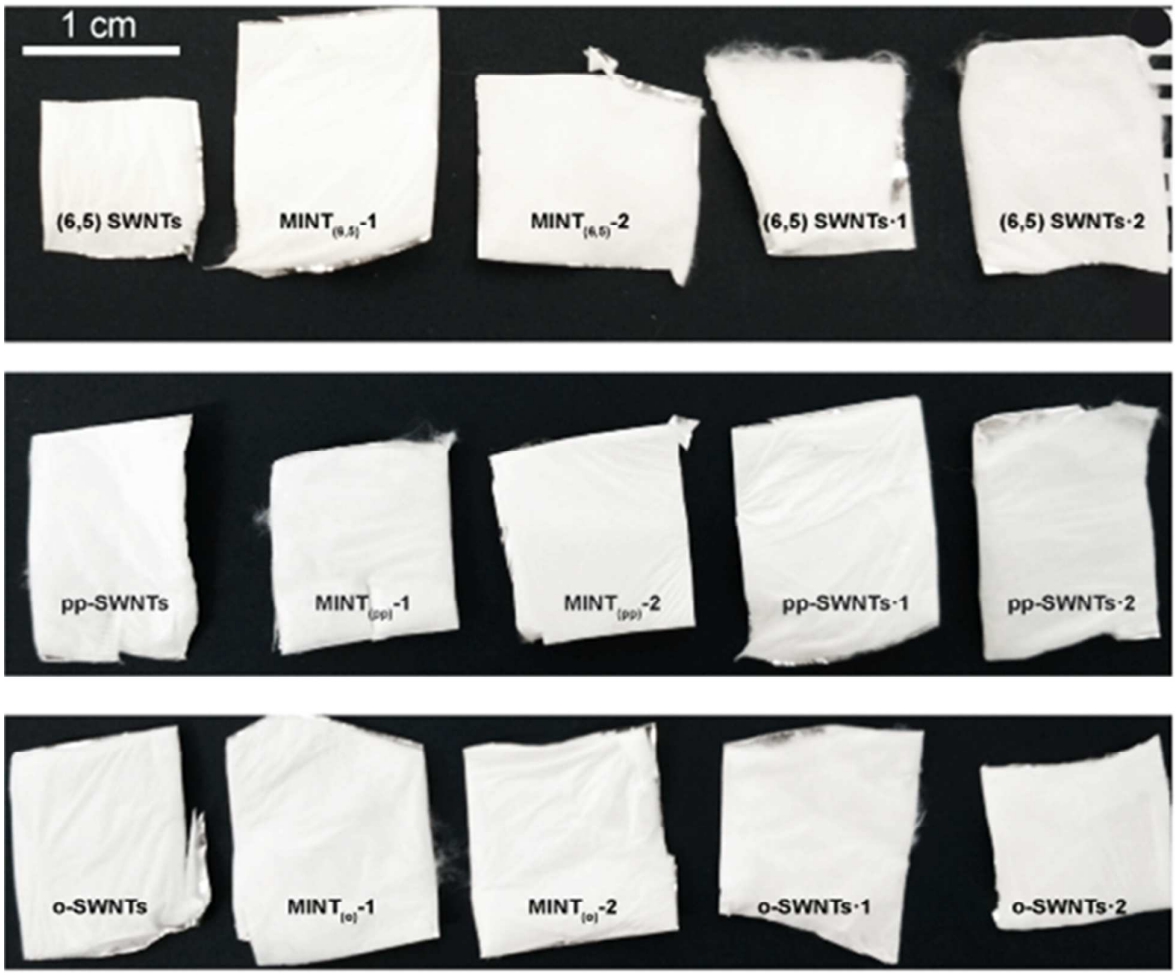

Figure S6. Samples of electrospun fibers. No macroscopic differences are observed.

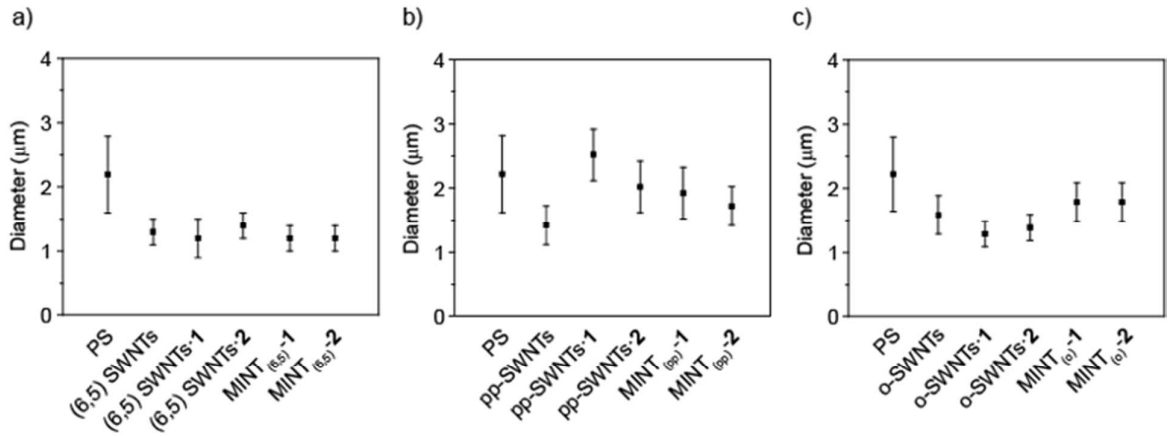

Figure S7. Diameter distribution of: a) (6,5) SWNTs samples; b) pp-SWNTs samples and c) o-SWNTs. Mean of 100 measurements.

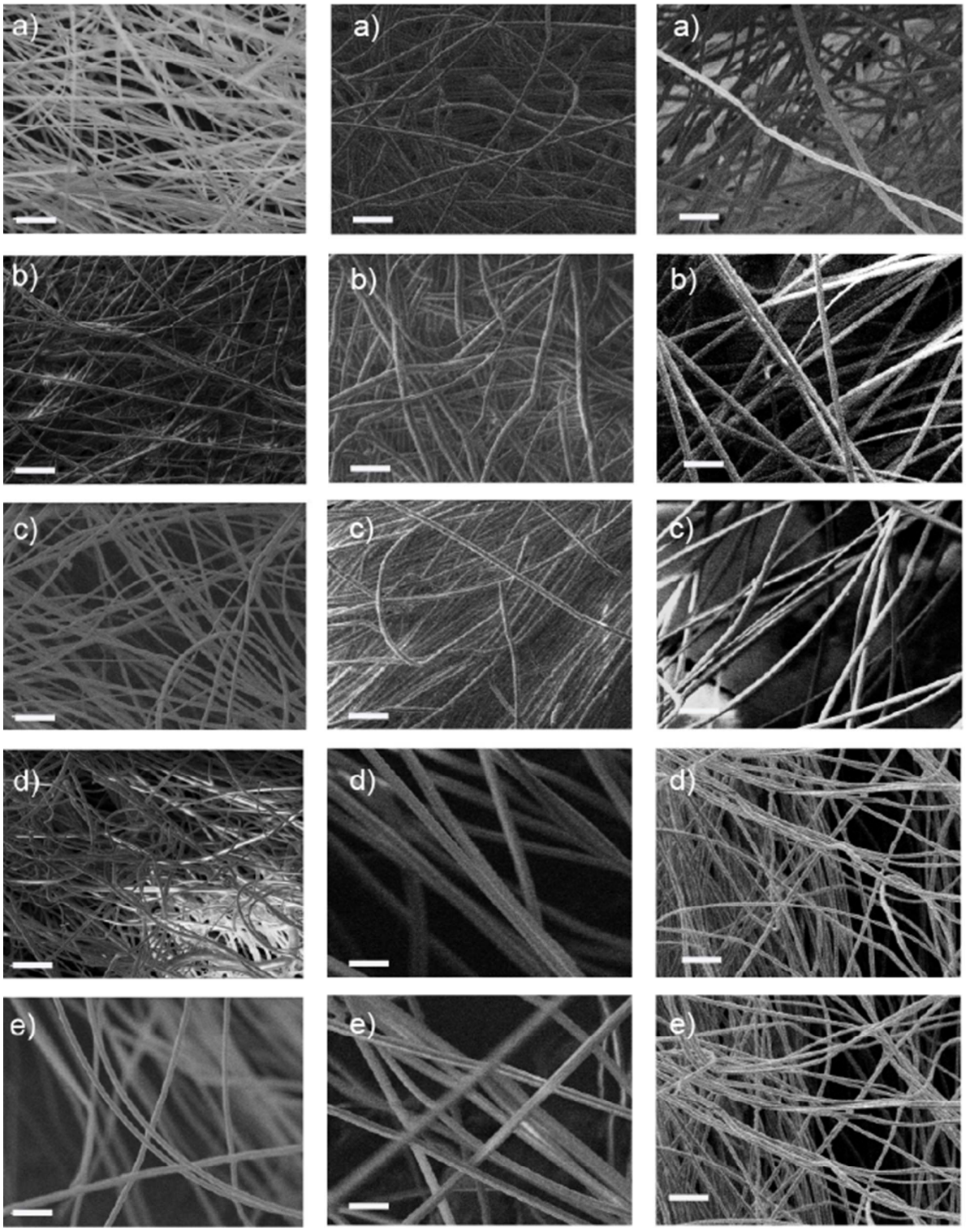

Figure S8. SEM images of (6,5)-SWNTs,pp-SWNTs and o-SWNTs samples. Left: a) (6,5)-SWNTs; b) $MINT_{(6,5)}$-**1**; c) $MINT_{(6,5)}$-**2**; d) (6,5) SWNTs-**1**; e) (6,5)-SWNTs-**2**. Center: a) pp-SWNTs; b) $MINT_{(pp)}$-**1**; c) $MINT_{(pp)}$-**2**; d) pp-SWNTs-**1**; e) pp-SWNTs-**2**. **Right:** a) o-SWNTs; b) $_{MINT(o)}$-**1**; c) $MINT_{(o)}$-**2**; d) o-SWNTs-**1**; e) o-SWNTs-**2.** Inset scale: 10 μm.

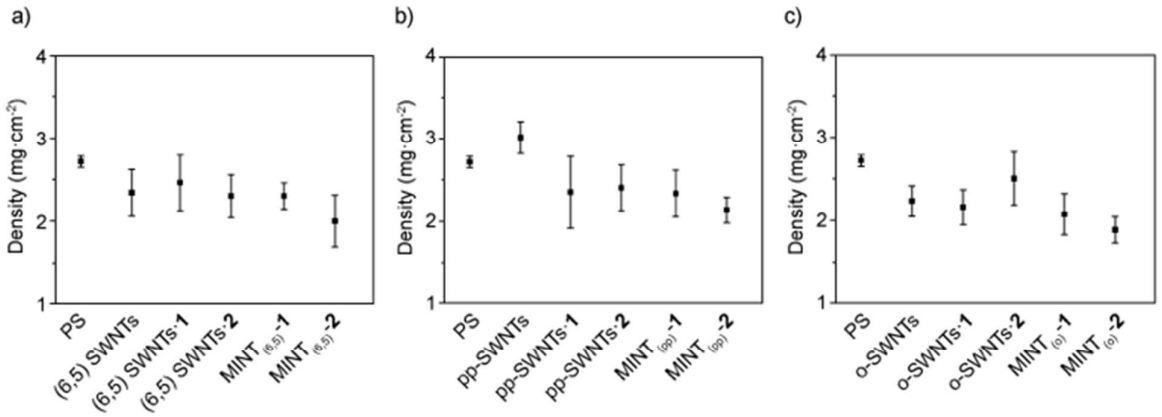

Figure S9. Fiber area density distribution: a) (6,5) SWNTs samples; b) pp-SWNTs samples and c) o-SWNTs. Mean of 7 measurements.

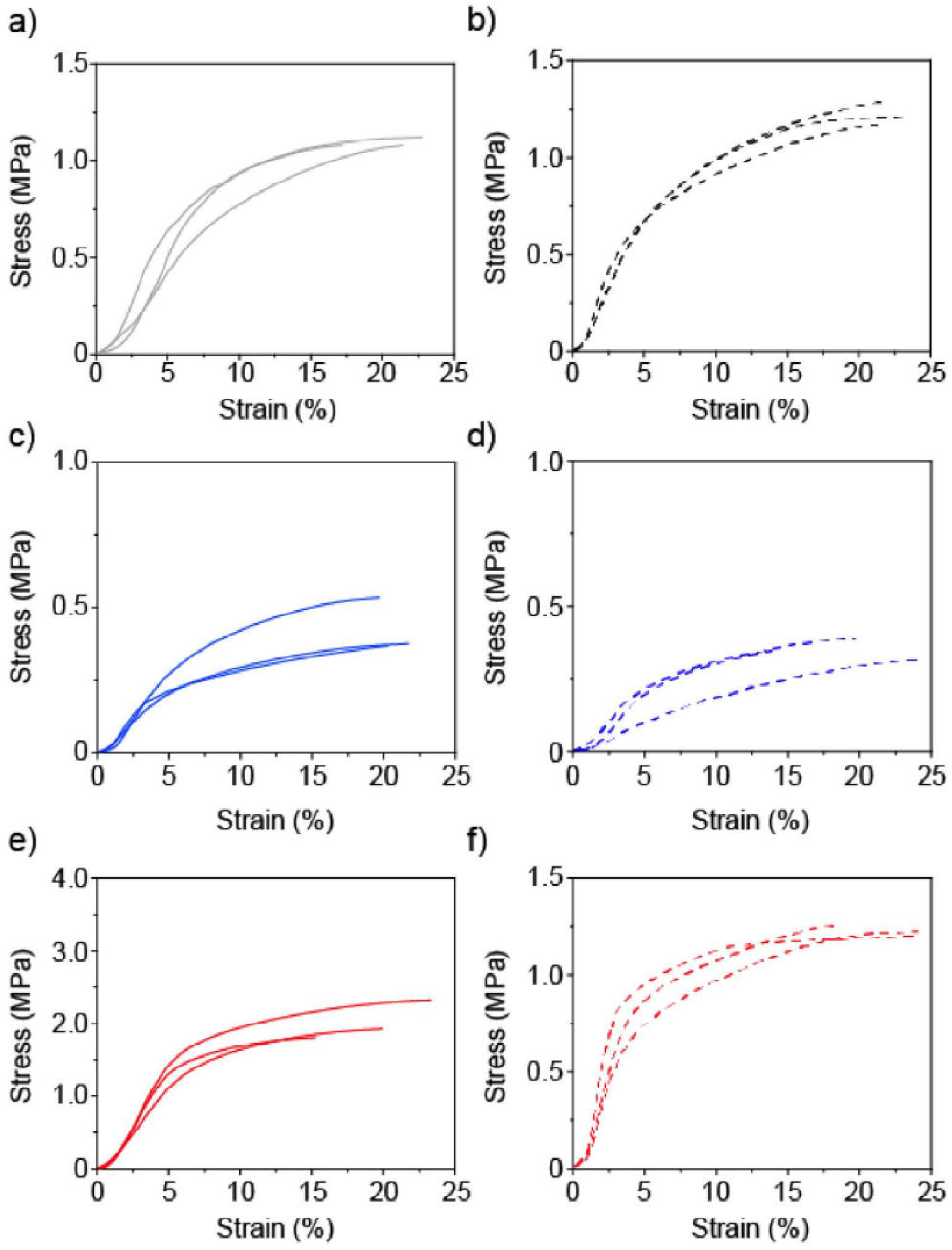

Figure S10. Stress/Strain curve of a) Polystyrene; b) (6,5)-SWNTs; c) (6,5)-SWNTs·**1**; d) (6,5)-SWNTs·**2**; e) $MINT_{(6,5)}$-**1** (red) f) $MINT_{(6,5)}$-**2**.

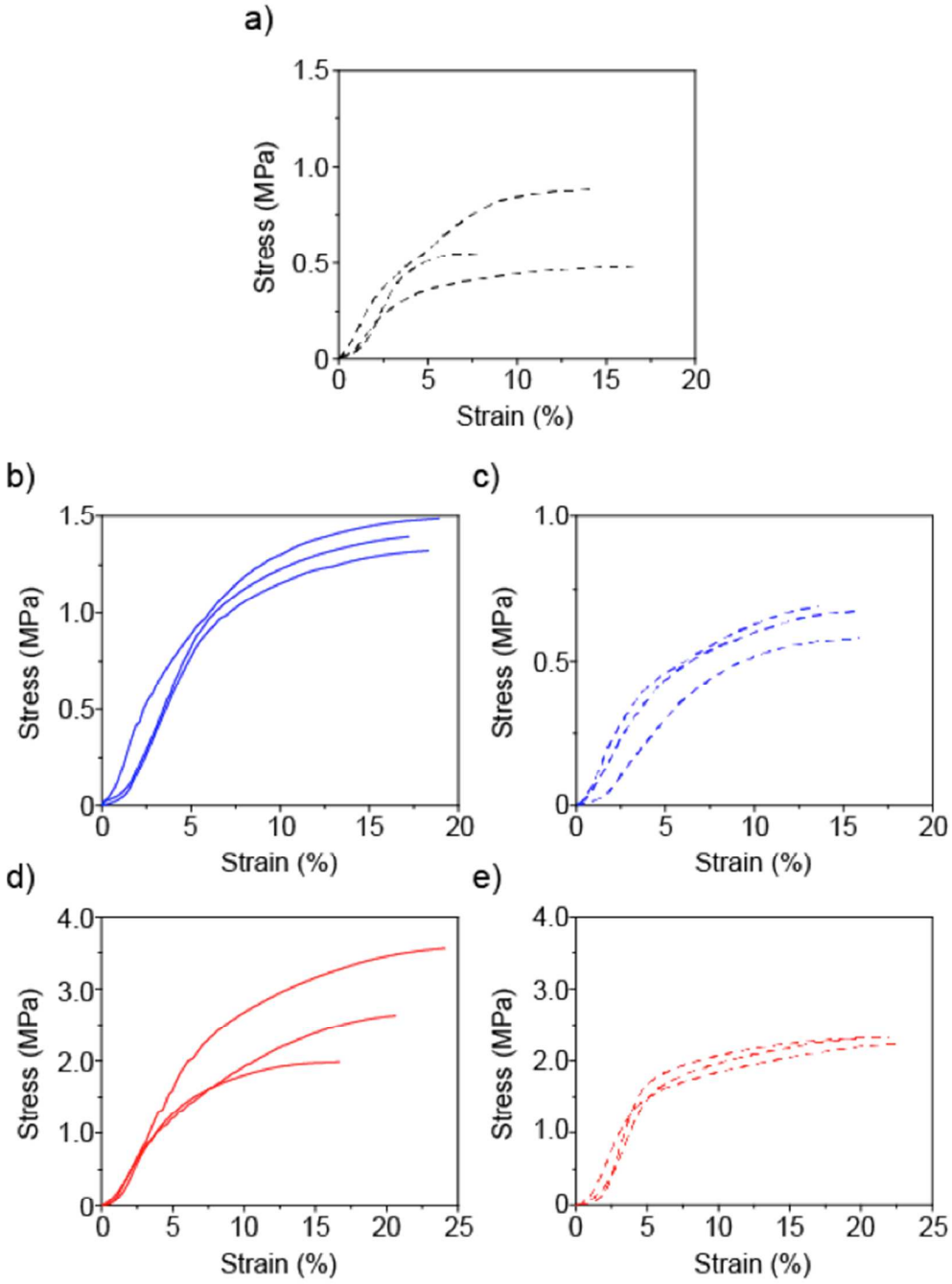

Figure S11. Stress/Strain curve of a) pp-SWNTs; b) pp-SWNTs·**1**; c) pp-SWNTs·**2**; d) $MINT_{(pp)}$-**1**; e) $MINT_{(pp)}$-**2**.

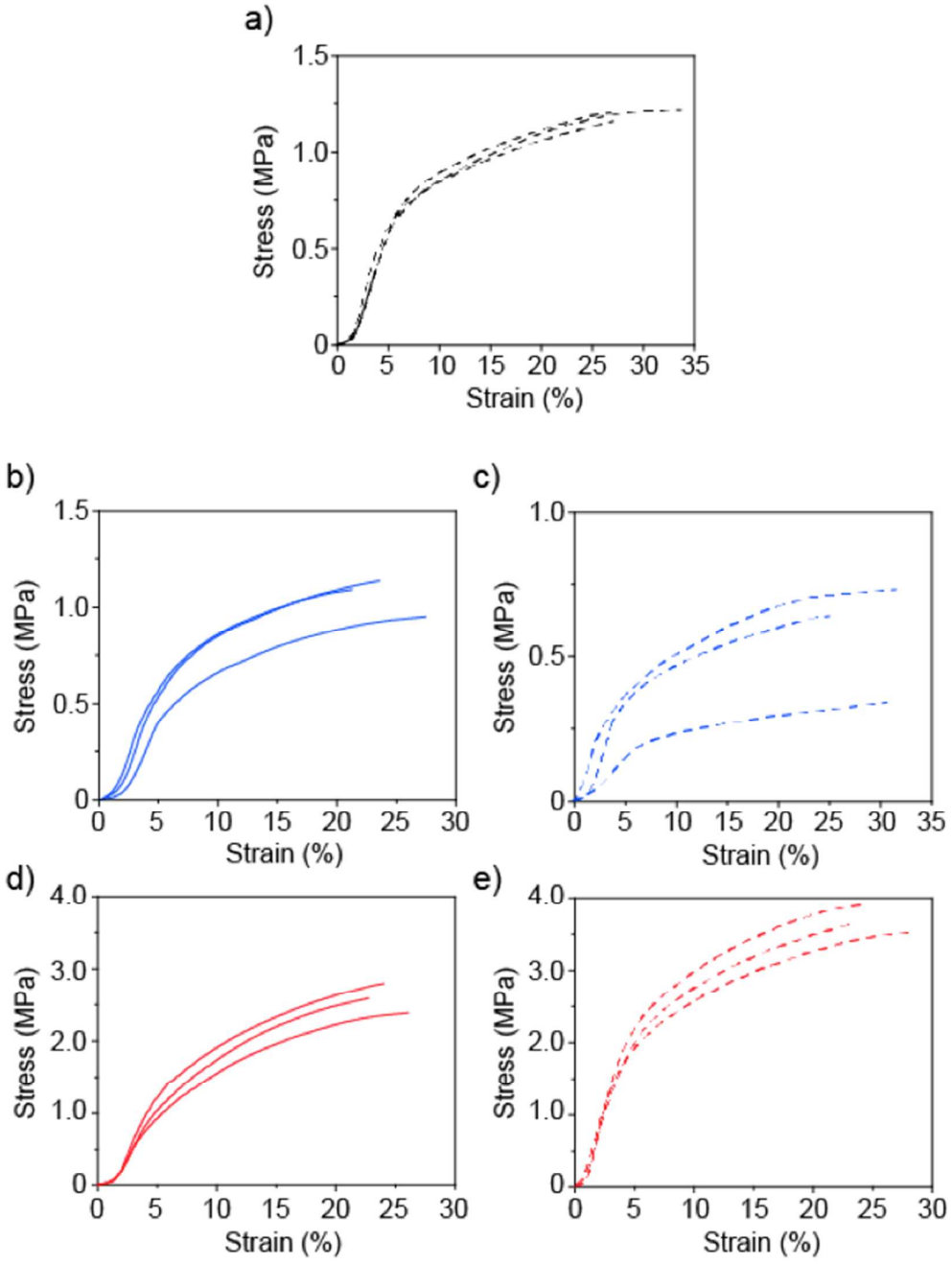

Figure S12. Stress/Strain curve of a) o-SWNTs; b) o-SWNTs·**1**; c) o-SWNTs·**2**; d) $MINT_{(o)}$-**1**; e) $MINT_{(o)}$-**2**.

Table S1. Young's Modulus and Tensile Strength in MPa of electrospun fibers.

Sample	Interaction	Young's Modulus /MPa	Tensile Strength /MPa	Variation of YM respect PS /%	Variation of TS respect PS /%
Polystyrene (PS)	-	15±1	1.09±0.03	-	-
PS/ (6,5)-SWNTs	-	18±1	1.26±0.06	20	16
PS/ MINT$_{(6,5)}$-**1**	Mechanical bond	32±6	2.0±0.3	110	80
PS/**1**·(6,5)-SWNTs	Supramolecular	7±1	0.39±0.03	-53	-60
PS/ MINT$_{(6,5)}$-**2**	Mechanical bond	21±7	1.18±0.08	40	8
PS/**2**·(6,5)-SWNTs	Supramolecular	6±1	0.37±0.05	-60	-66
PS/ pp-SWNTs	-	16±3	0.6±0.2	7	-40
PS/ MINT(pp)-**1**	Mechanical bond	34±5	3.0±0.7	130	170
PS/**1**·pp-SWNTs	Supramolecular	23±4	1.4±0.1	50	30
PS/ MINT$_{(pp)}$-**2**	Mechanical bond	50±12	2.25±0.05	230	106
PS/ **2**·pp-SWNTs	Supramolecular	11±3	0.65±0.06	-30	-40
PS/ o-SWNTs	-	23±2	1.18±0.02	50	8
PS/ MINT(o)-**1**	Mechanical bond	35±6	2.6±0.3	130	140
PS/ **1**· o-SWNTs	Supramolecular	19±7	1.4±0.6	30	30
PS/ MINT(o)-**2**	Mechanical bond	59±7	3.7±0.2	290	240
PS/ **2**· o-SWNTs	Supramolecular	10±4	0.6±0.2	-30	-40

Computational Methods

MD simulations were performed using AMBER 12 software package[1] for all calculations. Following the literature[2, 3] the AMBER99 force field[4] was used to model the SWNT, the polymer and the macrocycles **1** and **2**. For missing bonds, angle torsions, or Van Der Waals parameters not included in the AMBER99 force field, the values were transferred from the general AMBER force field (GAFF)[5]. The initial

structures were minimized using two cycles of conjugated gradient minimization. During the initial cycle, the SWNT was kept in their starting conformation using a harmonic constrains with a force constant of 500 Kcal/mol-Å. This was followed by another minimization cycle where the SWNT was kept a harmonic restraint force constant of 10 Kcal/mol-Å. To allow a slow relaxation of the systems: SWNT-polymer, supramolecular **1** and **2**, MINT **1** and **2**, the minimized structures was heated slowly from 0 to 300 K during 0.5 ns (using a 2 fs time step) under of constant-pressure-constant-temperature conditions (NPT). Finally, we carried out 5.0 ns (using a 2 fs time step) of MD simulation in NPT ensemble to equilibrate the system at 300 k. The positions of all SWNT atoms were constrained with a weak 10 Kcal/mol-Å harmonic potential during all MD simulation. In the figure **S.13** we show the calculated potential energy for all studied systems. We observe how the energy increases during the first few ps, corresponding to our heating process form 0 k to 300k, then the energy remains constant and the equilibrium was considered to be reached. Analysis and visualization of MD trajectories were performed with VMD software.[6] In the figure **S.14** we show the initial and the final state of the molecular dynamic simulations conducted.

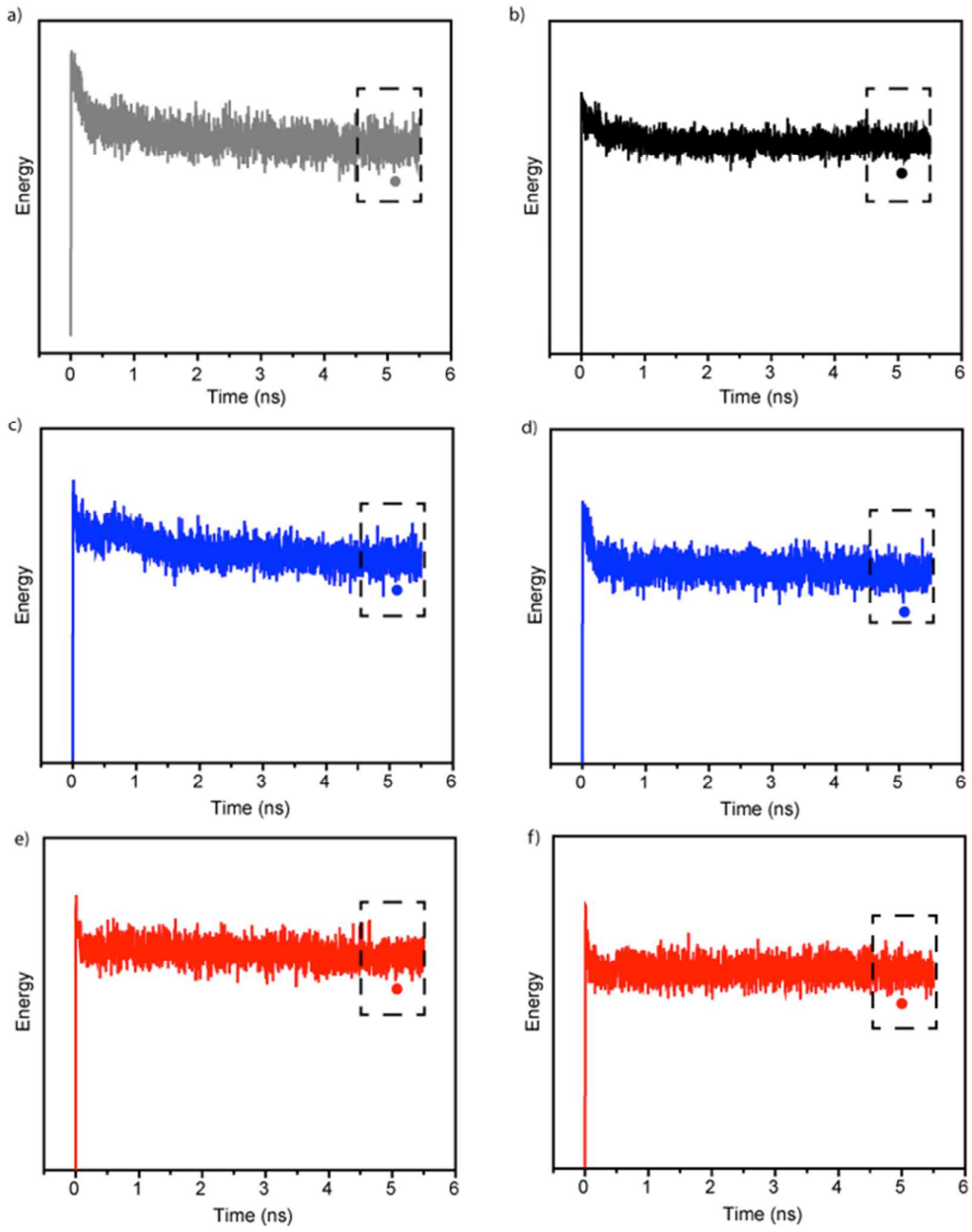

Figure S13. Stabilization energy of a) PS, and its composites with b) SWNTs, c) SWNT·**1,** d) SWNT·**2**, e) MINT-**1** and f) MINT-**2** during the 5.5 ns of MD simulations. The circles indicate the chosen structure for the figure 5. The dashed rectangles remark the chosen snap for the dihedral angle analysis.

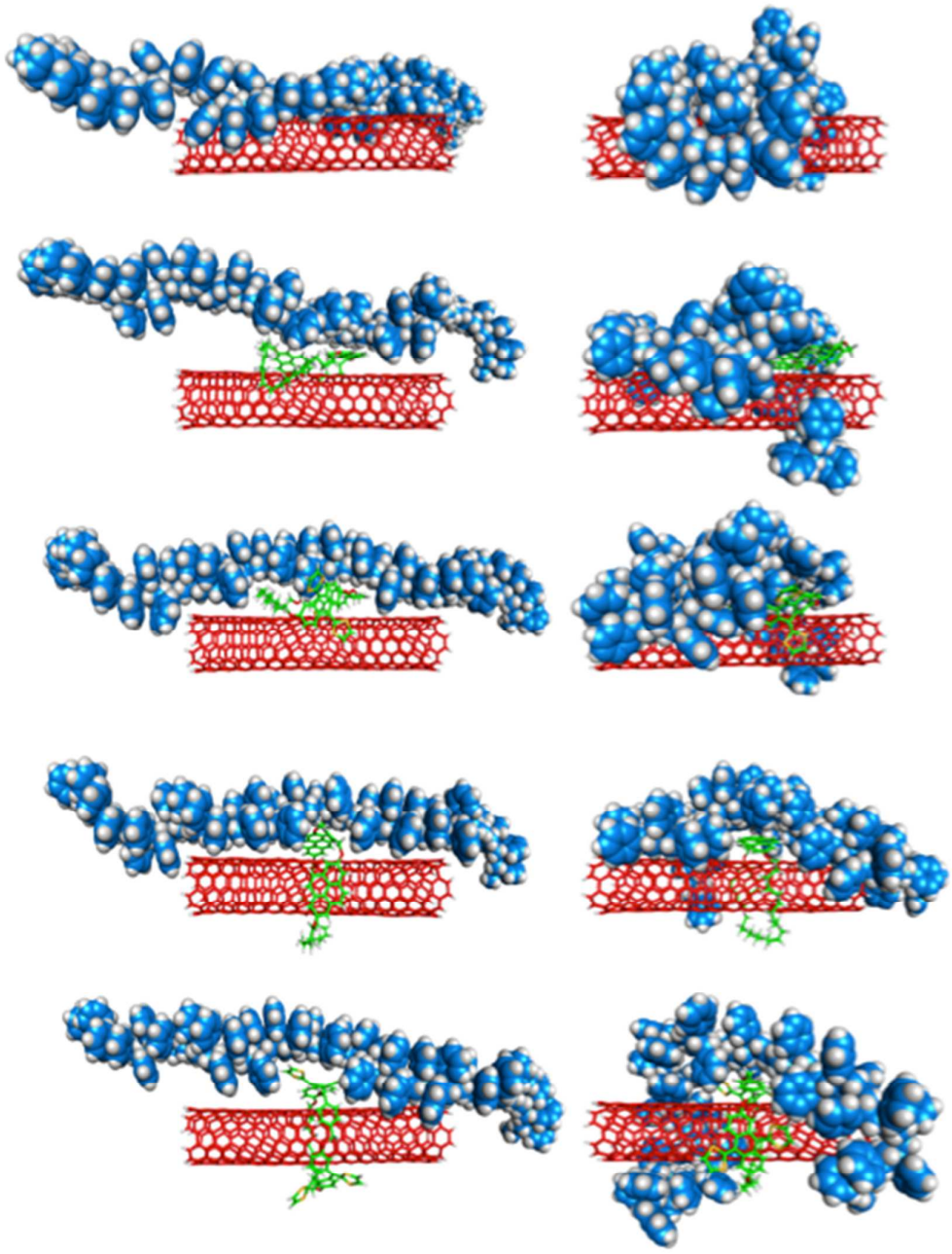

Figure S14. Initial and final state of the MD simulation for the five studied composites.

REFERENCES

1. Case, D.A.; Darden, T.A.; Cheatham, T.E.; III, Simmerling C.L.; Wang, J.; Duke, R.E.; Luo, R.; Walker, R.C.; Zhang, W.; Merz, K.M.; Roberts, B.; Hayik, S.; Roitberg, A.; Seabra, G.; Swails, J.; Götz, A.W.; Kolossváry, I.; Wong, K.F.; Paesani, F.; Vanicek, J., *et al.* AMBER 12. *University of California, San Francisco.* 2012.

2. Hummer, G.; Rasaiah, J. C.; Noworyta, J. P. Water Conduction Through the Hydrophobic Channel of a Carbon Nanotube. *Nature* **2001**, *414*, 188-190.

3. Johnson, R. R.; Johnson, A. T. C.; Klein, M. L. Probing the Structure of DNA−Carbon Nanotube Hybrids with Molecular Dynamics. *Nano Lett.* **2008**, *8*, 69-75.

4. Hornak, V.; Abel, R.; Okur, A.; Strockbine, B.; Roitberg, A.; Simmerling, C. Comparison of Multiple Amber Force Fields and Development of Improved Protein Backbone Parameters. *Proteins* **2006**, *65*, 712-725.

5. Wang, J.; Wolf, R. M.; Caldwell, J. W.; Kollman, P. A.; Case, D. A. Development and Testing of a General Amber Force Field. *J. Comput. Chem.* **2004**, *25*, 1157-1174.

6. Karplus, M.; McCammon, J. A. Molecular Dynamics Simulations of Biomolecules. *Nat. Struct. Biol.* **2002**, *9*, 646-652.